Effect of hydrogen on the structural and phase state and the deformation behavior of the ultrafine-grained Zr–1Nb alloy

Ekaterina N. Stepanova [a,*], Galina P. Grabovetskaya [b], Ivan P. Mishin [b]

[a] Institute of Physics and Technology at Tomsk Polytechnic University, Tomsk, Russia
[b] Institute of Strength Physics and Materials Science, Siberian Branch of the Russian Academy of Sciences, Tomsk, Russia

Keywords:
Hydrogen
Zirconium alloy
Ultrafine-grained structure
Deformation behavior

A B S T R A C T

The formation of an ultrafine-grained structure with predominantly high-angle grain boundaries and an average grain size of grain–subgrain structure elements of 0.4 μm in zirconium alloys was shown by electron microscopy and X-ray diffraction analysis. The formation of such structure was found to result in the significant increase of the ultimate and yield strengths in comparison with the initial fine-grained state. The strength characteristics of ultrafine-grained Zr–1Nb–0.22H alloy are higher than the corresponding characteristics of the Zr–1Nb alloy. The presence of hydrogen in the solid solution of the ultrafine-grained Zr–1Nb–0.22H alloy during tension at room temperature is found to prevent the development of plastic deformation localization on the meso- and macrolevels and to increase the effect of strain hardening and deformation of uniform extension. At elevated temperatures, the presence of hydrogen reduces the resistance to deformation localization on the macrolevel and the deformation to failure in tensile tests.

1. Introduction

Nowadays zirconium alloys possessing high biocompatibility and corrosion resistance are perspective materials for manufacturing medical implants [1]. Nevertheless, despite the high biocompatibility of zirconium alloys, their application for manufacturing medical implants is limited due to lower strength in comparison with titanium alloys and steel.

The formation of the ultrafine-grained (UFG) structure is known to be an effective method of improving the strength and operational characteristics of metal polycrystals at low homologous temperatures [2,3]. All most widely spread methods of the ultrafine-grained structure formation in metallic materials are based on Severe Plastic Deformation (SPD). The use of the SPD methods enables the sizes of the structural elements in the material to be decreased down to the nanolevel and, as a consequence, the strength characteristics to be increased by a factor of 1.5–2 [3]. At the same time, the rate of hydrogen absorption by metallic materials is well known to be increased with decreasing grain sizes. Therefore, the prospects for the application of the UFG polycrystals as structural materials will largely be determined by the evolution of deformation processes in the presence of hydrogen [3–5]. Taking into account the foregoing, the purpose of this work is to investigate the hydrogen effect on the structural and phase state, deformation behavior, and mechanical properties of the UFG Zr–1Nb alloy.

2. Experimental

Experiments were performed with the commercial Zr–1Nb alloy. In the initial state, the investigated alloy was heterophase one and had polycrystalline structure with grain sizes of 3–5 μm. The secondary phases in the form of round particles whose sizes varied from several tens of nanometers to several microns were located on the grain boundaries and in the bulk of the main Zr_α phase.

The UFG state of the alloy was obtained by compaction with the change of the deformation axis by two different methods. First, we used the method combining preliminary hydrogenation to concentration of 0.22% (hereinafter, the hydrogen concentration is indicated in weight percent) and triple compaction to 70–75% at temperatures 973–873 K [6]. The structure obtained was fixed by water quenching. The alloy was hydrogenated in gas media using a Siverst-type device at temperatures 973–873 K. The hydrogen concentration in the samples was measured by a RHEN 602 gas analyzer with ±0.0001% accuracy.

Second, to obtain the UFG state, compaction at room temperature with intermediate annealing at temperatures 873–803 K for 1 h was performed. The alloy was compacted in four cycles, each of which included triple pressing. Deformation after single pressing was 40–50%.

Thin foils were investigated using an EM-125K transmission electron microscope. The sizes of the structure elements were measured from micrographs by the secant method [7]. The volume fractions and the lattice parameters of phases were determined with accuracies of ±1% and 0.0001 nm, respectively, using a Shimadzu XRD7000 diffractometer with Cu Kα radiation source.

Tensile tests were performed at temperatures of 293 and 673 K in vacuum of 10^{-2} Pa using a PV-3012M machine equipped with a tensometric system of load measurement with automatic recording of flow curves in the load–time coordinates.

* Corresponding author.
E-mail address: enstepanova@tpu.ru (E.N. Stepanova).

Test specimens shaped as double blades were cut from billets by the electrospark method. Before testing, the specimen surfaces were subjected to mechanical grinding and electrolytic polishing.

3. Results and discussion

The typical electron micrographs and the corresponding electron diffraction patterns of the UFG structure of the Zr–1Nb alloy obtained by the method combining preliminary hydrogenation to 0.22% and hot plastic deformation by compaction to 70–75% is shown in Fig. 1. It is evident that an entangled deformational contrast is observed and some structure elements are poorly distinguished in the bright-field image of the structure. The electron diffraction patterns of the structure obtained for an area of 1.6 μm^2 show an appreciable number of reflections uniformly distributed over a circle with some of the reflections exhibiting azimuthal smearing (Fig. 2a). Such kind of electron diffraction patterns is characteristic for the UFG materials having high-angle misorientations of the structure elements, nonequilibrium grain boundaries, and internal fields of elastic stresses [8]. The average size of the grain–subgrain structure elements of the Zr–1Nb–0.22H alloy determined from the dark-field image (Fig. 2b) was (0.42 ± 0.1) μm.

X-ray structure investigations demonstrated that in addition to the main Zr_α phase of the UFG Zr–1Nb–0.22H alloy after compaction, it contains the secondary Nb(Zr) (bcc) phase (reflections 1 and 2 in Fig. 1c) as well as a certain amount of solid solution based on the Zr_α phase (reflection 4 in Fig. 1c). The electron microscopic studies also confirmed the presence of other phase precipitates in the volume of the main Zr_α phase (Fig. 1a). Furthermore, ZrH_86 and ZrH_2_225 hydrides whose reflections $(111)_{225}$, $(111)_{86}$, $(002)_{86}$, and $(220)_{86}$ were superimposed on the (101), (110), and (103) reflections of the Zr_α phase (Fig. 1c) were also detected in the alloy. It seems likely that some portion of hydrogen is present in the solid solution in the Zr_α phase. This is indicated by the increase of its lattice parameters in the Zr–1Nb–0.22 N alloy in comparison with the initial fine-grained state.

Compaction at room temperature with intermediate annealing also resulted in the formation of the UFG grain–subgrain structure (Fig. 2). However, in this case the UFG structure was less homogeneous. Along with areas that contained mostly elements with sizes of (0.1–0.4) μm, the structure comprised certain regions where the element sizes varied in the range (0.3–0.8) μm. The characteristics of the electron diffraction patterns and the dark-field image of such UFG structure indicated the presence of substantial misorientations between its elements (Fig. 2a and b). The average size of grain–subgrain structure elements of the UFG Zr–1Nb alloy calculated from the dark-field image was (0.45 ± 0.18) μm.

X-ray diffraction studies demonstrated the presence of Zr_α and Nb(Zr) phases and solid solution based on the Zr_α phase in the Zr–1Nb alloy after compaction at room temperature. Moreover, a certain amount of the Zr_β phase or solid solution on its basis (reflection 3 in Fig. 2c) was also contained in the alloy.

The typical tension curves for the UFG Zr–1Nb and Zr–1Nb–0.22H alloys (referred to as stress–strain curves below) at temperatures of 293 and 673 K are shown in Fig. 3 in the true stress–true strain coordinates. Generally, three deformation stages can be observed on the indicated curves: strain hardening, steady-state deformation, and declining stress. The duration of these deformation stages depended on the test temperature and the presence of hydrogen in the alloy.

At room temperature, the short strain hardening stage on the stress–strain curves of the UFG Zr–1Nb alloy is replaced by the sustained declining strain stage, in which two regions with different rates of strain decrease can be distinguished. The uniform deformation of the UFG Zr–1Nb alloy did not exceed 3%, while the total deformation to failure was about 18%. The short strain hardening stage and the low effect of strain hardening indicated the tendency toward strain localization on the macro level in the process of tension of the UFG Zr–1Nb alloy.

On the stress–strain curves for the UFG Zr–1Nb–0.22H alloy at 293 K, the three above-mentioned stages of deformation can be distinguished. Deformation achieved in the UFG Zr–1Nb–0.22H alloy during stages of strain hardening and steady-state deformation was ~10%, which was three times as large as in the UFG Zr–1Nb alloy. This indicates that the presence of hydrogen in the alloy reduces its tendency toward plastic strain localization on the macrolevel.

The testing temperature rise to 673 K leads to the appearance of the steady-state deformation stage on the stress–strain curve for the UFG Zr–1Nb alloy and approximately doubling of uniform deformation (curve 1′ in Fig. 3). The stress–strain curves of the UFG Zr–1Nb–0.22 N alloy demonstrate a decreasing duration of the strain hardening stages and reduction of the strain hardening

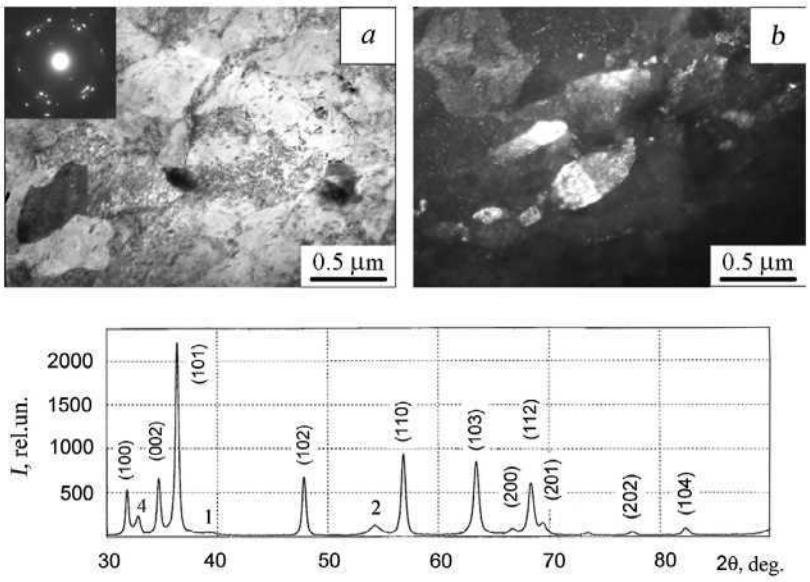

Fig. 1. UFG Zr–1Nb–0.22H alloy microstructure: (a) bright-field image, (b) dark-field image, and (c) fragment of the diffraction pattern.

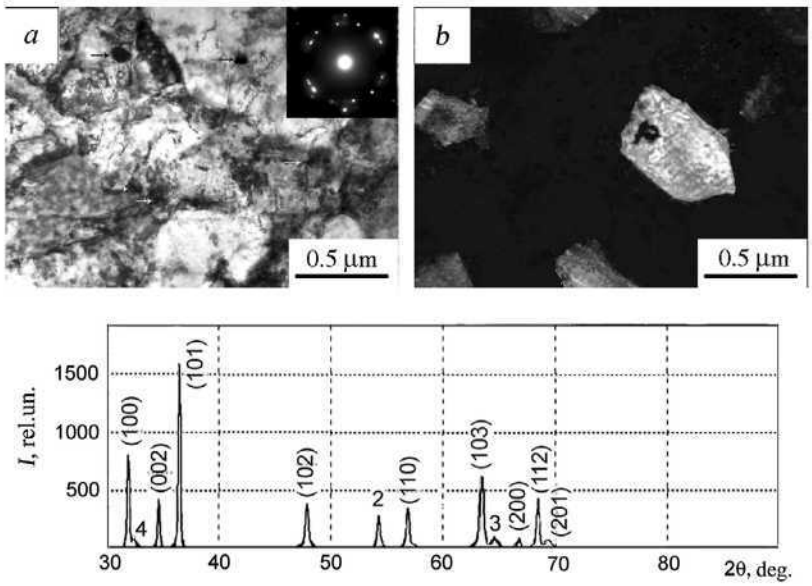

Fig. 2. UFG Zr–1Nb alloy microstructure (a) bright field image, (b) dark field image, and (c) fragment of the diffraction pattern. Alloy after compaction with change of deformation axis at room temperature with following annealing at 823 K for 1 h.

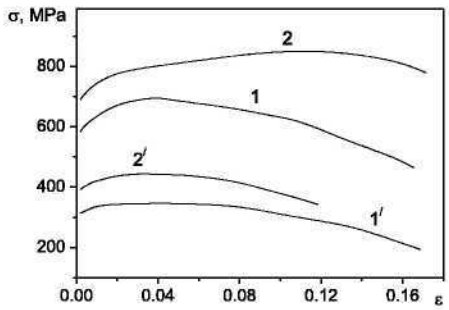

Fig. 3. True stress–true strain curves at temperatures of 293 (curves 1 and 2) and 673 K (curves 1′ and 2′). Here curves 1 and 1′ are for the UFG Zr–1Nb alloy, and curves 2 and 2′ are for the UFG Zr–1Nb–0.22H alloy.

effect with increasing temperature (curve 2′ in Fig. 3b). In addition, not only the value of uniform deformation decreases, but also the value of total deformation to failure reduces as compared to the UFG Zr–1Nb alloy. Conversely, the presence of hydrogen in the UFG Zr–1Nb alloy at elevated temperatures reduces its resistance to plastic tension strain localization on the macrolevel. This is confirmed by the results of studies of the preliminarily polished surface of the working part of the examined alloy samples.

During tension at room temperature, localized strain bands (mesobands) with widths of several microns were formed on the preliminary polished surface of the UFG Zr–1Nb alloy already in the strain-hardening stage. The mesobands of localized strain had intermittent character and were arranged at a small angle (0–15°) to the direction of load application. Strain localization on the macrolevel in this alloy had two stages. First, a clearly pronounced neck was formed, whose origin coincided with the beginning of the declining strain stage on the deformation curve. Then, along with the strain evolution in the neck, localized strain bands 0.2–0.3 mm wide appeared one after another at an angle of ~120° to one another (development of such bands in ultrafine-grained materials was considered in detail in [9]). No bands of localized strain were formed on the meso- and macrolevels in samples of the UFG Zr–1Nb–0.22H alloy during tension at room temperature. Pores and fine cracks were observed on the sample surfaces. Macroscale strain localization in this alloy occurred in the form of a weakly distinguished neck.

After tension at 673 K, no mesobands of localized strain were observed on the surface of the sample of the UFG Zr–1Nb alloy. At elevated temperature, strain localization on the macrolevel in the alloy proceeded through the formation of a clearly pronounced neck. In the UFG Zr–1Nb–0.22H alloy during tension at 673 K, deformation developed non-uniformly already in the strain hardening stage. Pores and small cracks were formed in some regions of the sample surface. Upon reaching the ultimate strength, the localized plastic strain bands appeared in the sample in which further deformation localization occurred.

Table 1 gives the strength and plastic characteristics of the UFG Zr–1Nb and Zr–1Nb–0.22H alloys. The mechanical properties of the Zr–1Nb alloy in the initial fine-grained state are also given here. A comparison of the mechanical properties demonstrates that the formation of the ultrafine-grained structure in the Zr–1Nb alloy leads to the increase (by 2–3 times) of the yield strength and the ultimate strength both at 293 and 673 K. The presence of hydrogen in the UFG Zr–1Nb alloy enhances the strength characteristics of the alloy, which is apparently due to solid solution hardening.

Table 1
Mechanical properties of a Zr–1Nb alloy in different states.

Test temperature (K)	Material	Yield strength (MPa)	Ultimate strength (MPa)	Uniform deformation (%)	Deformation to failure (%)
293	FG Zr–1Nb	300	300	17	34
	UFG Zr–1Nb	583	583	2.5	18
	UFG Zr–1Nb–0.22H	688	688	10	19
673	FG Zr–1Nb	114	114	30	48
	UFG Zr–1Nb	313	313	6	18
	UFG Zr–1Nb–0.22H	393	393	3.5	14

4. Conclusions

Thus, the formation of an ultrafine-grained structure in the Zr–1Nb alloy leads to a significant (by 2–3 times) increase of its ultimate strength and yield strength with simultaneous decrease of uniform deformation and deformation to failure. The presence of hydrogen in the UFG Zr–1Nb alloy prevents the development of plastic strain localization on meso- and macrolevels during tension at room temperature and increases the strain hardening effect and uniform extension deformation. During tension at elevated temperatures, the presence of hydrogen in the UFG Zr–1Nb alloy promotes the reduction of the alloy resistance to strain localization on the macrolevel and decreases the uniform extension deformation and deformation to failure.

Acknowledgements

This work was performed with the use of equipment of the Tomsk Center for Collective Use in Materials Science and was supported by the Russian Foundation for Basic Research (Project No. 13-02-98007).

References

[1] M. Fujita, J. Jpn. Stomatol. Soc. 60 (1) (1993) 54.
[2] D.G. Morris, Mechanical Behavior of Nanostructured Materials, Trans. Tech. Publication Ltd., Switzerland, 1998. p. 85.
[3] E.N. Stepanova, G.P. Grabovetskaya, O.V. Zabudchenko, I.P. Mishin, Russ. Phys. J. 54 (6) (2011) 690–696.
[4] G.P. Grabovetskaya, E.N. Stepanova, I.V. Ratochka, E.V. Naidenkin, O.N. Lykova, Inorg. Mater.: Appl. Res. 4 (2) (2013) 92–97.
[5] F.H. Froes, O.N. Senkov, J.I. Qazi, J. Int. Mater. Rev. 49 (3) (2004) 227–245.
[6] E.N. Stepanova, G.P. Grabovetskaya, I.P. Mishin, K.A. Prosolov, J. Int. Sci. Public.: Mater. Methods Technol. 7 (Part 1) (2013) 178–186.
[7] S.A. Saltikov, Stereometric metallography [in Russian], Metallurgy, Moscow, 1970. p. 375.
[8] Yu.R. Kolobov, R.Z. Valiev, G.P. Grabovetskaya, A.P. Zhilyaev, E.F. Dudarev, K.V. Ivanov, M.B. Ivanov, O.A. Kashin, E.V. Naidenkin, Grain Boundary Diffusion and Properties of Nanostructured Materials [in Russian], Nauka, Novosibirsk, 2001. p. 213.
[9] E.V. Naydenkin, G.P. Grabovetskaya, J. Mater. Sci. Forum. 633–634 (2010) 107–119.